Optical and microwave properties of metal–ammonia solutions*

Morrel H. Cohen

James Franck Institute and Department of Physics, The University of Chicago, Chicago, Illinois 60637

Itzhak Webman and Joshua Jortner

Department of Chemistry, Tel-Aviv University, Tel-Aviv, Israel
(Received 19 August 1975)

In this paper we present an analysis of the optical and microwave properties of metal–ammonia solutions in the concentration range 2–9 MPM. The analysis rests on the physical picture of a continuous metal–nonmetal transition, intermediated by microscopic inhomogeneities originating from bimodal concentration fluctuations. Effective-medium theory for the complex dielectric constant gives a good account of the optical properties of Li—NH_3 in the energy range 0.6–1.4 eV. On the other hand, effective-medium theory is inadequate for the microwave properties, and results of numerical simulation are presented.

I. INTRODUCTION

A physical picture was recently advanced[1,2] for the continuous metal–nonmetal transition in metal–ammonia solutions (MAS)[3–6] in the intermediate concentration range $M = 1-9$ MPM, proposing that in Li–NH_3 and in Na–NH_3 solutions a metallic regime is separated from a nonmetallic one by a microscopically inhomogeneous regime in which concentration fluctuations determine the local electronic structure and the transport properties. It was further proposed[1,2] that the concentration fluctuations in this system are bimodally distributed, with the metal concentration fluctuating locally about either of the well defined values M_0 and M_1, where $M_0 > M_1$ and with the local concentration remaining near M_0 or M_1 over radii which are approximately equal to the correlation length b for concentration fluctuations. Provided that the Ornstein–Zernike decay length for concentration fluctuations is much smaller than b, a percolation problem can be defined in which a volume fraction C of the material is occupied by metallic regions of concentration M_0, with the remainder containing the nonmetallic component of concentration M_1. M_0 and M_1 are the upper and the lower limits of the inhomogeneous regime, respectively, while C depends linearly on M. Furthermore, provided that the phase coherence length of the conduction electrons is shorter than b and tunneling corrections are negligible, one can define local electronic structure and transport properties. The limits of the inhomogeneous regime were determined from a combination of concentration fluctuation measurements, electrical conductivity, Hall effect, and paramagnetic susceptibility data to be $M_0 = 9$ MPM and $M_1 = 2.3$ MPM, giving the C scale,

$$C \cong (3M - 7)/20 , \tag{1.1}$$

for both Li–NH_3 at 223 K and Na–NH_3 at 240 K. This model has been successful[2] in providing a quantitative analysis of the electrical and the thermal transport properties of MAS in the inhomogeneous regime, establishing the self-consistency of our physical picture.

We emphasize, however, that the proposed bimodal distribution of concentration fluctuations in MAS is not yet borne out by direct experimental evidence. The analysis of chemical potential data by Ichikawa and Thompson[7] for Li–NH_3 and Na–NH_3 solutions does provide evidence for large concentration fluctuations, but does not reveal, in particular, whether they are bimodally or unimodally distributed. Similarly, the recent small-angle neutron scattering data of Chieux[8] for Li–NH_3 solutions were analyzed in terms of the Ornstein–Zernike picture, resulting in a decay length of the form $70\,|T - T_c|^{-1/2}$ Å with T and T_c in K, where T_c is the consolute temperature for Li–NH_3 solutions. Chieux's[8] study was conducted at 4 MPM, near the critical concentration, where ordinary critical fluctuations may be superposed upon the bimodal distribution proposed by us. It is, however, improbable that critical concentration fluctuations will prevail throughout the whole concentration range of 2.3–9 MPM, within which the chemical potential data show large fluctuations to exist. Ultrasonic attenuation data of Bowen,[9] in fact, do show evidence for critical fluctuations near the consolute point superposed on a broad background of concentration fluctuations which are weakly temperature independent.

Accordingly, we are continuing our program of analyzing data on the basis of our model of MAS. In the present paper we study the optical and the microwave properties in the intermediate concentration range. For the former we utilize the EMT; for the latter we use the results of numerical simulations. Agreement with the optical data is good, providing further support for the existence of an inhomogeneous regime in this system. A theory of microwave properties is presented. Uncertainty over the experimental data, however, prevents a meaningful comparison with the theory.

II. EFFECTIVE MEDIUM THEORY FOR THE OPTICAL PROPERTIES

We have developed[10] an effective-medium theory[11–14] (EMT) for the frequency-dependent dielectric constant $\epsilon(\omega)$ of a microscopically inhomogeneous material such as we have proposed[1,2] MAS to be between 2.3 and 9.0 MPM. The EMT condition for $\epsilon(\omega)$ is

$$\left\langle \frac{\epsilon(\omega) - \epsilon^i(\omega)}{2\epsilon(\omega) + \epsilon^i(\omega)} \right\rangle = 0 , \tag{2.1}$$

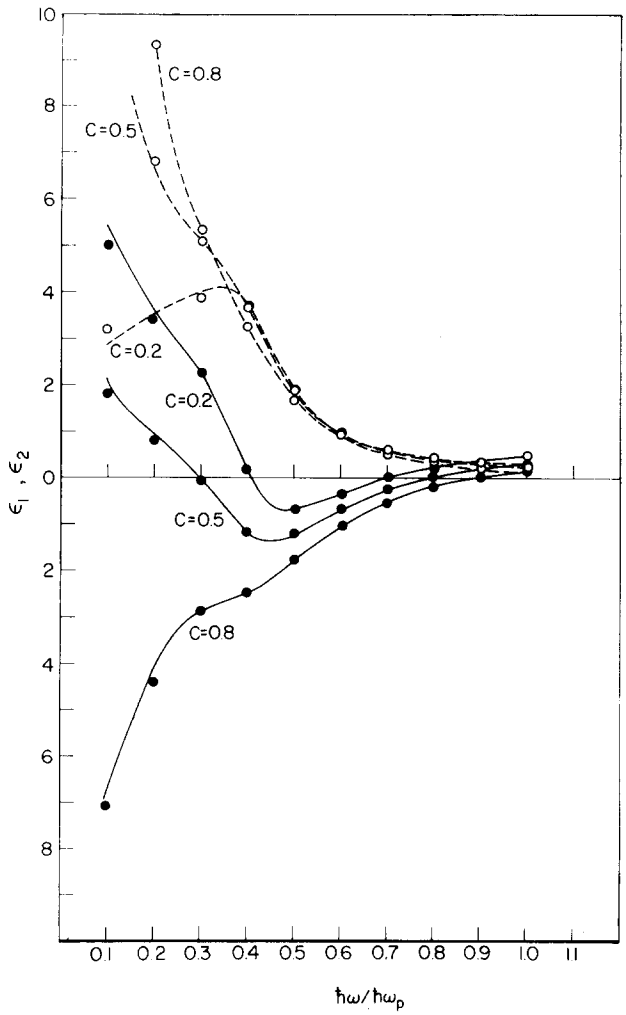

FIG. 1. Results of model calculations of the optical properties of a microscopically inhomogeneous system, with a bimodal distribution of metallic regions. The complex dielectric function $\epsilon^0(\omega)$ for the metallic regions (with probability C) and $\epsilon^1(\omega)$ for the nonmetallic regions (with $1-C$) is given by Eq. (2.7). —— ϵ_1(EMT); ● ϵ_1—numerical simulations for a 8×8×8 s.c. network, - - - - - ϵ_2(EMT); o ϵ_2—numerical simulations for a 8×8×8 s.c. network.

where $\epsilon^i(\omega)$ is a possible value of the local complex dielectric function and the average is over all such values. In the present case $\epsilon^i(\omega)$ takes on a functional form $\epsilon^0(\omega)$, characteristic of the metallic regions, with probability C or $\epsilon^1(\omega)$, characteristic of the nonmetallic regions, with probability $1-C$, so that Eq. (2.1) becomes

$$C\left(\frac{\epsilon(\omega)-\epsilon^0(\omega)}{2\epsilon(\omega)+\epsilon^0(\omega)}\right)+(1-C)\left(\frac{\epsilon(\omega)-\epsilon^1(\omega)}{2\epsilon(\omega)+\epsilon^1(\omega)}\right)=0\ . \tag{2.2}$$

These equations may be readily solved to yield explicit results for $\epsilon(\omega)$:

$$\epsilon(\omega)=\epsilon_1(\omega)+i\epsilon_2(\omega)=\epsilon^0(\omega)f[C,\ x(\omega)]\ , \tag{2.3}$$

$$f(C,\ x(\omega))=a(\omega)\pm\sqrt{[a(\omega)]^2+\tfrac{1}{2}x(\omega)}\ , \tag{2.4}$$

$$a(\omega)=\tfrac{1}{2}\left[(\tfrac{3}{2}C-\tfrac{1}{2})(1-x(\omega)+\tfrac{1}{2}x(\omega)\right]\ , \tag{2.5}$$

$$x(\omega)=\epsilon^1(\omega)/\epsilon^0(\omega)\ . \tag{2.6}$$

The sign is chosen in (2.4) to give positive $\epsilon_2(\omega) = \mathrm{Im}[\epsilon(\omega)]$. Equations (2.3)–(2.6) represent the generalization of the EMT for a real, diagonal, second-order tensor[15] to the complex case.[10] Our experience with the former case[14,16] leads us to expect that Eqs. (2.3)–(2.6) are accurate for all values of C if $|x(\omega)|$ is within the range 0.03–30. Numerical simulations of $\epsilon(\omega)$ in a s.c. network bear out this expectation. In Fig. 1 we present typical results for a two-component model system where the optical properties of the metallic regions correspond to the Drude form, while the complex dielectric function in the nonmetallic regions is given in terms of a single resonance, so that

$$\epsilon^0(\omega)=1-\frac{\omega_p^2}{\omega(\omega+i/\tau)}$$

$$\epsilon^1(\omega)=1-\frac{f_L}{(\omega^2-\omega_0^2)+i\omega\Gamma}\ . \tag{2.7}$$

The metallic regions are characterized by the plasma frequency ω_p and the relaxation time τ with $\omega_p\tau=4.0$, while the nonmetallic regions are specified by the oscillator strength $f_i\,\omega_p^{-2}=0.6$, the resonance frequency by $\omega_0/\omega_p=0.40$, and the resonance width by $\Gamma/\omega_p=0.25$. As is evident from Fig. 1 the results of the numerical simulations for the optical properties[10] practically coincide with the EMT. In the case of inhomogeneous MAS the condition $0.03\lesssim|x(\omega)|\lesssim 30$ is well met at optical frequencies. Accordingly, in the next section we fit the optical data for Li–NH_3 solutions to the EMT.

III. OPTICAL PROPERTIES OF METAL-AMMONIA SOLUTIONS

The first study of the optical reflectivity of Na–NH_3 solutions was conducted by Beckman and Pitzer,[17] who observed a reflectivity peak at 0.8–0.76 eV for metal concentrations below $M=5$ MPM and a nearly Drude–Lorentz type behavior for higher values of M. More detailed studies of the optical constants of Na–NH_3 and Li–NH_3 were carried out by Thompson and his colleagues.[18–20] At concentrations above 8–10 MPM, $\epsilon_1(\omega)$ and $\epsilon_2(\omega)$ differ only in details from the behavior expected for a Drude, free-electron system. In the concentration range 8–2 MPM, which corresponds approximately to the inhomogeneous regime, $\epsilon_1(\omega)$ exhibits a continuous variation from metallic towards resonance behavior, characteristic of a very broad resonance located at about 0.6 eV. This is consistent with the behavior of $\epsilon_2(\omega)$, which is Drude-like and shows a slow variation with M in the range above 4–8 MPM with an indication of resonance behavior around 0.6 eV at 2–3 MPM. At much lower concentrations optical absorption data reveal a well defined resonance which has been attributed to the $1s\rightarrow 2p$ transition of the solvated electron within its cavity. As the concentration increases up to 0.5 MPM the position of the resonance shifts from 0.8 eV in the dilute limit to 0.7 eV without broadening. It is therefore probable that the absorption evident in $\epsilon_2(\omega)$ above 0.6 eV for 2 MPM is the high-energy half of the same cavity resonance shifted down in energy to 0.6 eV and substantially broadened, in agreement with Thompson and colleagues.[18,19] The latter also point out that there are signs of persistence of this bound-electron absorption to substantial-

ly higher concentrations, (6 MPM). This mixed behavior of the optical properties is consistent with our model for microscopic inhomogeneities in these solutions in that concentration range and it lends further weight to our attempts to fit the optical data to the EMT. The shift from 0.8 towards 0.7 eV starts at about 10^{-3} MPM, the same concentration at which the equivalent conductance starts decreasing. The latter decrease is associated with solvated electron–solvated ion pairing. The wavelength shift is therefore most probably associated with a downward shift of a p state relative to the s state caused by the cation. It is of considerable interest that no further shift or broadening probably occurs until beyond 1 MPM, i.e., a shift from 0.7 to 0.6 eV and an increase in linewidth from 0.4 to 0.6 eV occurs between 1 and 2 MPM. We have argued elsewhere[2] that the electron–cation complexes characteristic of the electrolyte solutions with $M > 10^{-3}$ MPM start dissociating at 0.1 MPM. A fused-salt structure starts forming somewhere between 0.1 and 1 MPM. Significant overlap of electronic wavefunctions in neighboring cavities sets in at 1 MPM and is responsible for the onset of spin paramagnetism and the dramatic increase in the conductivity. The transport properties, however, remain nonmetallic in the range 1–2 MPM. The electronic wavefunctions remain localized, and a Mott transition does not occur. The optical absorption is entirely consistent with this picture. Increasing overlap between cavity states is responsible for the shift and broadening, but the continuing localized character of the states (localized in the Anderson sense) is responsible for the persistence of the resonance.

The most extensive data for MAS in the relevant concentration range are available[18] for Li–NH_3 solutions at 213 K (i.e., $T - T_c = 3.5$ K) and these experimental results were analyzed in terms of our model. In the comparison between the EMT and the data, the first task is to establish values for $\epsilon^0(\omega)$ and $\epsilon^1(\omega)$. Unfortunately, values for $\epsilon(\omega)$ are unavailable at the limits of the inhomogeneous regime, and we were forced to use indirect means to establish $\epsilon^0(\omega)$ and $\epsilon^1(\omega)$ for Li–NH_3 solutions. We chose a Drude–Lorentz form for $\epsilon^0(\omega)$,

$$\epsilon^0(\omega) = \epsilon_\infty - \frac{\omega_p^2}{\omega(\omega + i/\tau)} \tag{3.1}$$

the three parameters ϵ_∞, $\hbar\omega p$, and τ were subsequently

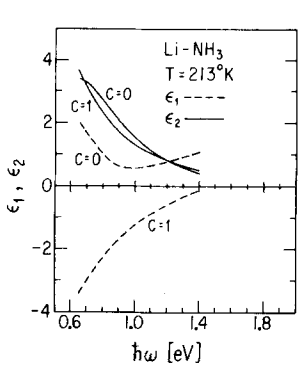

FIG. 2. $\epsilon^0(\omega)$ and $\epsilon^1(\omega)$ for Li–NH_3 solutions.

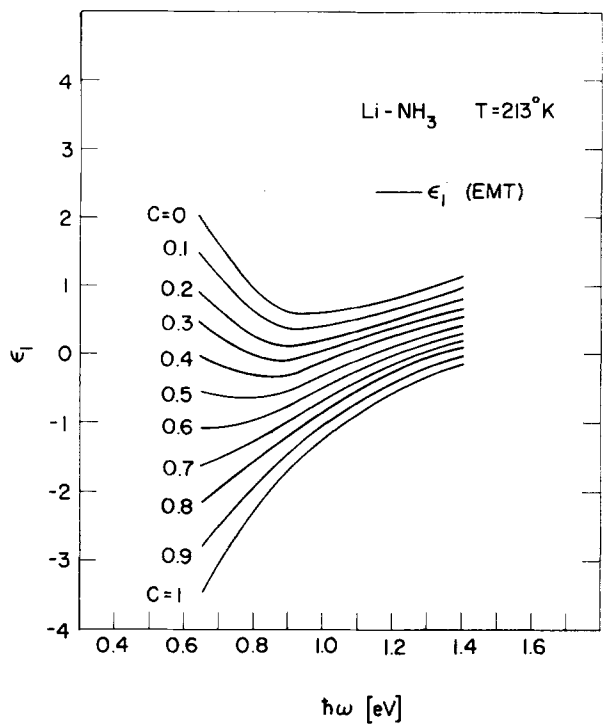

FIG. 3. The dependence of $\epsilon_1(\omega)$ on C for Li–NH_3.

determined by fitting the Drude form (3.1) to the data for 12 MPM. Thompson and Cronenwett[18] had interpreted their data at 8 and 12 MPM in terms of the Drude model, and the concentration dependence of their parameters was used as a guide in selecting final values at 9 MPM:

$$\epsilon_\infty = 1.35\ ,$$
$$\hbar\omega_p = 1.8\ \text{eV}\ ,$$
$$\hbar/\tau = 0.5\ \text{eV}\ . \tag{3.2}$$

$\epsilon^1(\omega)$ was determined by inserting (3.2) and the experimental values of $\epsilon(\omega)$ into (2.3)–(2.6) for $M = 3$ MPM (i.e., $C = 0.1$) and solving for $\epsilon^1(\omega)$. The results for $\epsilon^0(\omega)$ and $\epsilon^1(\omega)$ are shown in Fig. 2. The variation of $\epsilon_1(\omega)$ with C, Fig. 3, exhibits the expected transition from the Drude free-electron type behavior to a resonance behavior at about $C \simeq 0.6$, which according to Eq. (1.1) corresponds to $M \simeq 6.3$ MPM for Li–NH_3. This value of C will be slightly dependent on $\epsilon^1(\omega)$ and on $\epsilon_2(\omega)$, and we assert that in general this transition from Drude type behavior to resonance behavior will occur in the range $C = 0.5$–0.6. Next, calculations of $\epsilon(\omega)$ were made for $M = 4$ MPM ($C = 0.25$), $M = 5$ MPM ($C = 0.4$), and $M = 8$ MPM ($C = 0.85$) in Li–NH_3. Comparisons of the EMT and the experimental data for $\epsilon_1(\omega)$ and for $\epsilon_2(\omega)$ are shown in Figs. 4 and 5. The agreement between theory and experiment for $\epsilon_1(\omega)$ is excellent throughout. Some improvement in the agreement between $\epsilon_2(\omega)$ for the 8 MPM solution could be obtained by modifying the Drude–Lorentz parameters slightly, otherwise the agreement with $\epsilon_2(\omega)$ is good. In view of the satisfactory fit of $\epsilon_1(\omega)$ and $\epsilon_2(\omega)$ with the EMT the energy loss functions, $-\text{Im}[\epsilon(\omega)^{-1}]$, are adequately accounted for, as is evident from Fig. 6.

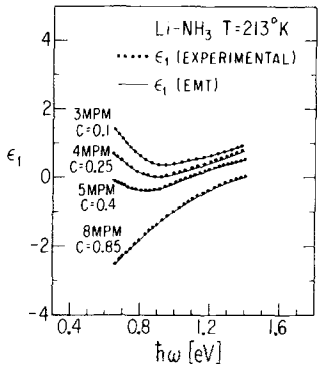

FIG. 4. Concentration dependence of $\epsilon_1(\omega)$ for Li–NH_3 solutions at 213 K. Experimental data from Ref. 17.

The available experimental data for ^{19}Na–NH_3 at $T = 230$ K (i.e., $T - T_c \simeq 3$ K) recorded at concentrations of 2 MPM, 5 MPM, 6 MPM, and 8 MPM are qualitatively similar to those for Li–NH_3. It is interesting to note that $\epsilon_1(\omega)$ derived for Li–NH_3, Fig. 2, is similar to $\epsilon(\omega)$ for Na–NH_3 in its frequency dependence. Scaling $\epsilon_1(\omega)$ and $\epsilon_2(\omega)$ for 2 MPM Na–NH_3 by a factor of 0.62–0.72 brings the two curves into near coincidence. In view of absence of experimental information concerning $\epsilon^1(\omega)$ for Na–NH_3 which may differ quite appreciably from the value of $\epsilon(\omega)$ at 2 MPM, we have refrained from a detailed analysis of the data. We note that the transition from Drude type behavior to resonance behavior for $\epsilon_1(\omega)$ in Na–NH_3 solutions occurs at the concentration range 6–5 MPM, which corresponds to $C \simeq 0.5$, in qualitative agreement with the predictions of our model of microscopic inhomogeneities in this system.

We therefore believe that, as emphasized by Thompson and colleagues,[18,19] bound-electron absorption persists well into the intermediate range and that this persistence is strong evidence for compositional inhomogeneities within that range. The analysis of the optical data supports our physical picture that these compositional inhomogeneities are of the bimodal type. If the inhomogeneities were unimodal, $\epsilon_1^1(\omega)$ would vary considerably with local composition. While it is possible

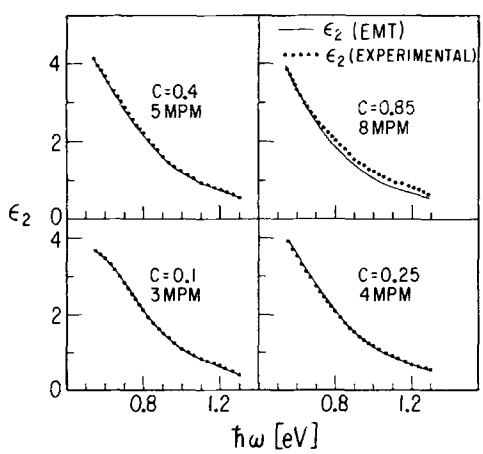

FIG. 5. Concentration dependence of $\epsilon_2(\omega)$ for Li–NH_3 solutions at 213 K. Experimental data from Ref. 17.

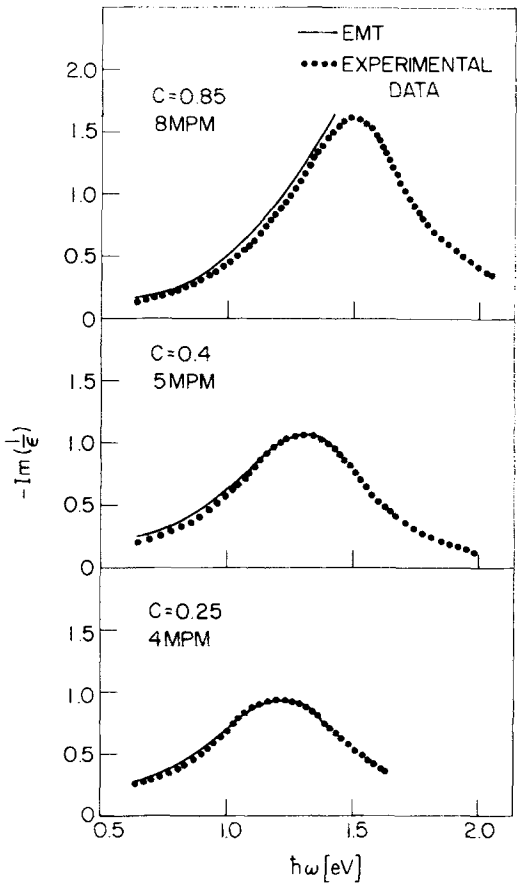

FIG. 6. Concentration dependence of the loss function $-\mathrm{Im}(1/\epsilon)$ for Li–NH_3 solutions.

to recast the EMT for unimodally distributed fluctuations into a binary form,[21] a Drude form for $\epsilon^0(\omega)$ would not be indicated, in particular as regards $\epsilon_1^0(\omega)$. The good fit obtained for the rapidly varying quantity, $\epsilon_1(\omega)$, therefore reinforces the assumption of bimodality.

One could ignore the possibilities of inhomogeneities of either kind, and interpret the metal–nonmetal transition in MAS as a smeared out Mott transition.[22] Persistence of the electron cavity resonance would then be explained as the development of an atomic transition into an interband transition. In our opinion, the line would broaden too rapidly in the transition region for this to be the case. Suppose the ions and cavities to be in a fused-salt-like structure. The linewidth would have a contribution from electron–atom interactions which is 0.4 eV for the isolated cavity. Assuming breakdown of k-selection rules, it would have another contribution approximately equal to the sum of the widths of the s and p bands and substantially greater than twice the s-band width. This latter contribution would be increased further by the positional disorder of the electron cavities. At the Mott transition, the s-band width would be about equal to the electron–electron interaction U in the Hubbard model. The best available estimate of U comes from O'Reilly's[23] and Logan and Kestner's[24] studies of the stability of the dielectron cavity, about 0.2 eV. Thus, at the Mott transition, the linewidth must be substantially greater than

0.8 eV and probably at least 1.2 eV. This is too large to account for the observed persistence into the transition region.

IV. MICROWAVE PROPERTIES OF METAL-AMMONIA SOLUTIONS

The complex microwave dielectric constant of Na–NH_3 solutions at 10 GHz was studied by Mahaffey and Jerde,[25] who reported a dramatic concentration dependence of $\epsilon_1(\omega)$. At low metal concentrations up to 10^{-1} MPM they find $\epsilon_1 \simeq 20$, which is close to the static dielectric constant of pure NH_3. In the range $10^{-1} - 1$ MPM ϵ_1 increases from 20 to 30 with increasing metal concentration. Above 1 MPM ϵ_1 increases more rapidly, reaching the value of ~100 at 2.5 MPM and then dropping abruptly to negative values. $\epsilon_1 = 0$ at 2.8 MPM at 230 K. At the upper limit of the inhomogeneous regime $M = 9$ MPM ϵ_1 reaches -1.5×10^4. This variation of ϵ_1 from $+10^2$ to $\sim -10^4$ over the inhomogeneous regime implies that EMT cannot be used for $\epsilon(\omega)$; numerical simulation is necessary.

Cohen and Jortner have proposed[2] that in the range 10^{-1}–1 MPM, small complexes of solvated ions and electrons break up in a gradual transition towards a fused salt structure. In such a structure there would be an extra contribution to $\epsilon_1(\omega)$ for small ω analogous to the difference between ϵ_0 and ϵ_∞ in an ionic crystal. We therefore attribute the observed increase of ϵ_1 from 20 to 38 in this range to dissociation and incipient formation of a fused salt structure. We have also pointed out that the increase in spin susceptibility and conductivity between 1 and 2.3 MPM implies that the electronic states are beginning to extend over more than one cavity. In such a case, there is an electronic contribution to the dielectric constant of the form $4\pi N\alpha$, with N being the solvated-electron number density and α proportional to the cube of the electronic localization length L.[26] We attribute the observed increase of ϵ_1 from 38 to 100 in the range 1 to 2.5 MPM to this spreading of the electronic wavefunctions. The subsequent variation in ϵ_1 through zero to large negative numbers as M increases is a reflection of the metal–nonmetal transition.

At 9 MPM, a value of 75 for ϵ_2 was observed. These data for ϵ_1 and ϵ_2 at the lower limit of the homogeneous propagation regime are incompatible with Drude–Lorentz behavior at low frequencies, where Eq. (3.1) results in

$$\epsilon_1^0(\omega \to 0) = \epsilon_\infty - (\omega_p/\gamma)$$
$$\epsilon_2^0(\omega \to 0) = \omega_p^2/\omega\gamma \,. \tag{4.1}$$

Utilizing the parameters derived from the analysis of the optical data, Eq. (3.2) we choose $\epsilon_\infty = 1.35$, $\omega_p = 1.8$ eV, and $\hbar\gamma = 0.5\hbar/\tau = 0.3$ eV; the factor 0.5 in the last quantity accounts for the difference between the optical relaxation time and that corresponding to the dc conductivity, as recommended by Sommoans and Thompson.[19] Eq. (4.1) with these parameters results in $\epsilon_1^0 = -34.6$ and $\epsilon_2^0 = 2.8\times10^5$ at 10 GHz ($\hbar\omega = 3.9\times10^{-5}$ eV). There is little resemblance between these estimates, which rest on the Drude model, and the experimental data at 9 MPM, $\epsilon_1^0 = -1.7\times10^4$ and $\epsilon_2^0 = 75$. Mahaffey and Jerde[25] have already noted the serious discrepancy between their experimental results for ϵ_2 in the concentration range 5–10 MPM and the dc conductivity data. In the concentration range 1–5 MPM the dc conductivity is equal to $\omega\epsilon_0\epsilon_2$, where ϵ_0 is a proportionality constant. On the other hand, at 9 MPM the dc conductivity exceeds $\omega\epsilon_0\epsilon_2$ by about one order of magnitude. These serious discrepancies between the optical measurements extrapolated via the Drude–Lorentz theory and the microwave measurements raise doubts about the latter.

In view of these uncertainties there is no reliable way to extract the values of ϵ^0 and ϵ^1 at the limits of the inhomogeneous regime which are required as input data for our theoretical analysis. There are two alternative routes to follow. First, we can assert that the Drude model is quantitatively inapplicable for the description of the metallic regimes and Eq. (3.1) just provides a convenient two parameter interpolation formula for $\epsilon^0(\omega)$ in the optical region. The corresponding values of the parameters required as input data for the microwave complex dielectric constant are then taken from experiment. Alternatively, we can assert that the microwave data are incorrect and use the Drude–Lorentz theory to obtain the required input data by extrapolation from the optical data. We shall follow both routes in the hope that subsequent microwave measurements will clear away the uncertainties. We start with the former route and use the experimental values.

$$\epsilon_1^0 = -1.7\times10^4\,, \quad \epsilon_2^0 = 75 \qquad 9 \text{ MPM}$$
$$\epsilon_1^1 = 40\,, \qquad \epsilon_2^1 = 5 \qquad 2.3 \text{ MPM}\,. \tag{4.2}$$

Numerical studies of dc conductivity in cubic networks[12,15] have established that the EMT is accurate for $0.4 < C < 1$ for all values of the conductivity ratio between the nonmetallic and the metallic regions, while serious deviations from the EMT are exhibited for low values (<0.03) of the conductivity ratio for $C < 0.4$. This is not surprising as the EMT overestimates the value of the percolation threshold C^*, $C^*_{\text{EMT}} = \frac{1}{3}$, whereas $C^* \cong 0.17$ for the continuous percolation problem. We expect that a similar state of affairs will prevail for the complex dielectric function. In the present case $|\epsilon_1^1/\epsilon_1^0| = 2.1\times10^{-3}$ and $\epsilon_2^1/\epsilon_2^0 \sim 1$ so that the EMT is inadequate for $C < 0.4$ for the microwave $\epsilon(\omega)$ in MAS. In order to mimic the features of the continuum percolation problem we have performed numerical simulations of $\epsilon(\omega)$ in a cubic network with correlated bonds. In doing so we have utilized the numerical procedure developed by us. In view of convergence problems encountered in the numerical simulations of $\epsilon(\omega)$ for large networks we were limited to $8\times8\times8$ networks, where the convergence was adequate. The recent numerical studies of Skal[27] on the percolation probability in s.c. networks demonstrate that numerical simulations for surprisingly small $5\times5\times5$ networks yields C^* to an accuracy of 10%. Our network size limited us in extending the range of bond correlation, and we have limited ourselves to incorporating correlation between nearest neighbors only. The results of the numerical simulations are shown in Figs. 7 and 8 for

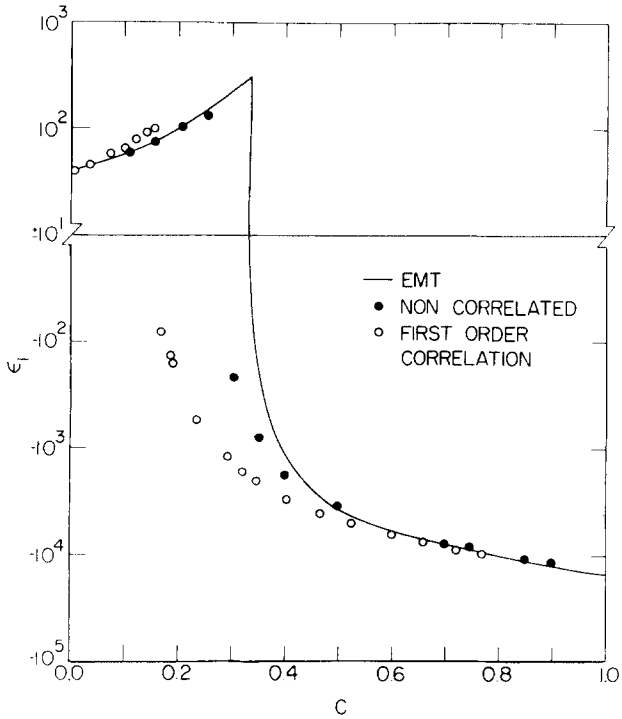

FIG. 7. Results of numerical simulations for the real part of the microwave dielectric constant. $\epsilon^1(\omega)$ and $\epsilon^0(\omega)$ are given in terms of Eq. (4.2). The calculations were performed for a $8\times8\times8$ network without and with bond correlation between metallic bonds. Closed circles (●): noncorrelated bonds. Open circles (○): nearest neighbor correlation between metallic bonds. Solid Curve: EMT result.

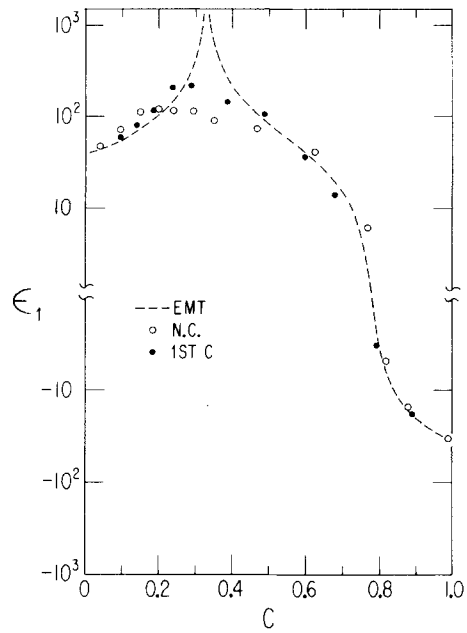

FIG. 9. Results of numerical simulations for the real part of the microwave dielectric constant for a model system where $\epsilon^1(\omega)$ is given by (4.2) while $\epsilon^0(\omega)$ is given by the Drude parameters of Eq. (4.3). ● numerical simulations for a $8\times8\times8$ s.c. network. ○ numerical simulations for a $8\times8\times8$ s.c. network with nearest neighbor correlation between metallic bonds. solid line: EMT.

the parameters given by Eq. (4.2). The solid curves correspond to the EMT, curve 1 representing the results of the numerical simulations without bond correlation and curve 2 incorporates nearest neighbor bond correlation. The behavior of ϵ_2, Fig. 8, is identical with that expected for the dc conductivity. The dependence of ϵ_1 on C exhibits an initial rise at low C values followed by a dramatic drop to low negative values. For the EMT $\epsilon_1=0$ at $C=0.33$, for the noncorrelated s.c. network $\epsilon_1=0$ at $C=0.25$, while for the case of the s.c. network with nearest neighbor correlation ϵ_1 vanishes at $C=0.17$.[16] Thus for an inhomogeneous material characterized by a low negative value of $\epsilon_1^1/\epsilon_1^0$ the real part of the microwave dielectric constant vanishes at the percolation threshold.

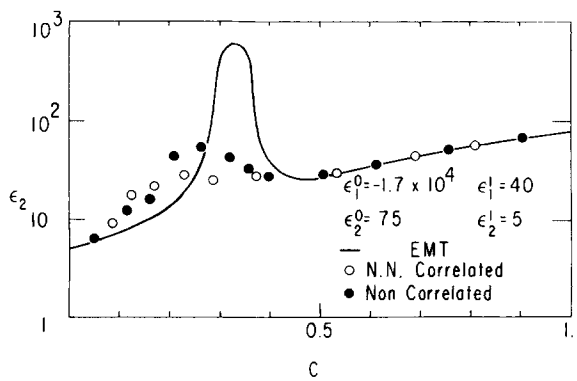

FIG. 8. Results of numerical simulations for the imaginary part of the microwave dielectric constant. $\epsilon^1(\omega)$ and $\epsilon^0(\omega)$ from Eq. (4.2). Details of calculations and presentation of results identical with those for Fig. 7.

We have compared the experimental data with the results of numerical simulation for a s.c. network with nearest neighbor correlations. The concentration dependence of ϵ_1, Fig. 7, exhibits the striking features revealed by the experimental data.[25]

In view of the uncertainty over the experimental data, there is little point at present to improve the theory by introducing corrections due to boundary scattering effects as we have done in the analysis of the dc conductivity data. Moreover, we believe that the extrapolation of the optical data to microwave frequencies via the Drude–Lorentz theory provides at least equally valid input data:

$$\epsilon_1^0=-34.5\,,\quad \epsilon_2^0=2.8\times10^5\,. \tag{4.3}$$

Values of ϵ_1^1 and ϵ_2^1 are those given in (4.2). The corresponding ratios are $|\epsilon_1^1/\epsilon_1^0|=1$ and $|\epsilon_2^1/\epsilon_2^0|=1.3\times10^{-4}$ so that effective medium theory cannot be used below $C=0.4$. The results are shown in Figs. 9 and 10.

For low C, ϵ_1 rises as for the previous case. It increases at low C values exhibiting a broad maximum around $C=0.3$. It vanishes around $C=0.78$ beyond which it is negative (metallic). The results of numerical simulation with and without nearest neighbor correlation agree well with each other and with the EMT except for a spurious peak in the EMT at $C=0.33$ which is absent in the simulations. The value of C at which ϵ_1 vanishes has now been shown to depend on the value of ϵ_1^0. When the latter is sufficiently negative, as for

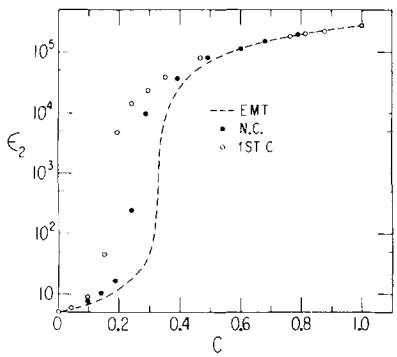

FIG. 10. Results of numerical simulations of the imaginary part of the microwave dielectric constant for the model system of Fig. 9. Input data, details of calculations and presentation of results identical to those of Fig. 9.

the experimental ϵ^0, ϵ_1 appears from our calculations to vanish at C^*, whereas for the Drude values of ϵ^0, ϵ_1 vanishes at $C = 0.78$. In Fig. 10, the value of C at which $\epsilon_2(\omega)$ drops precipitously moves towards the percolation threshold $C^* = 0.17$ as EMT is replaced by the network simulation without and with bond correlations, just as for the dc conductivity.[5]

V. CONCLUSIONS

Our model of bimodal concentration fluctuations in MAS accounts well for the optical data on Li solutions in the range 2–10 MPM, providing further support for the applicability of the model. The microwave data are too uncertain for conclusions to be drawn from them. However, our analysis of those data and of an extrapolation to microwave frequencies of the optical data shows that once the experimental uncertainties are resolved, the microwave dielectric constant should provide useful supplementary information on the state of MAS in the transition region. In particular, because the ratio $|\epsilon_1^1/\epsilon_1^0|$ or $|\epsilon_2^1/\epsilon_2^0|$ can lie well outside the range of validity of EMT, numerical simulations are necessary for $C < 0.4$. These are sensitive to the difference between unimodal and bimodal distributions of $\epsilon(\omega)$ and can be used as a test of our hypothesis of bimodality.

*This research has been supported in part by the U.S.A.–Israel Binational Science Foundation at the Tel-Aviv University. We have also benefited from support by the ARO(D), and by the Louis Block Fund and the Materials Research Laboratory of the National Science Foundation at The University of Chicago.

[1]Morrel H. Cohen and J. Jortner, J. Chem. Phys. 58, 5170 (1973).
[2]J. Jortner and Morrel H. Cohen, Phys. Rev. (in press).
[3]*Metal Ammonia Solutions*, edited by G. Lepoutre and M. J. Sienko (Benjamin, New York, 1964).
[4]*Metal Ammonia Solutions*, edited by J. J. Lagowski and M. J. Sienko (Buttersworth, London, 1970).
[5]*Electrons in Fluids*, Proc. of Colloque Weyl III on Metal Ammonia Solutions, edited by J. Jortner and N. R. Kestner (Springer-Verlag, Heidelberg, 1973).
[6]Morrel H. Cohen and J. C. Thompson, Adv. Phys. 17, 857 (1968).
[7]K. Ichikawa and J. C. Thompson, J. Chem. Phys. 59, 1680 (1973).
[8]P. Chieux, Phys. Lett. A 48, 493 (1974).
[9]D. E. Bowen, Phys. Lett. A 51, 207 (1975).
[10]I. Webman, J. Jortner, and M. H. Cohen (unpublished).
[11]D. A. G. Bruggeman, Ann. Phys. (Leipzig) 24, 636 (1935).
[12]R. Landauer, J. Appl. Phys. 23, 779 (1952).
[13]H. J. Juretschke, R. Landauer, and J. A. Swanson, J. Appl. Phys. 27, 838 (1956).
[14]S. Kirkpatrick, Phys. Rev. Lett. 27, 1722 (1971).
[15]Morrel H. Cohen and J. Jortner, Phys. Rev. Lett. 30, 696 (1973).
[16]I. Webman, J. Jortner, and Morrel H. Cohen, Phys. Rev. B 11, 2885 (1975).
[17]T. A. Beckman and K. S. Pitzer, J. Phys. Chem. 65, 1527 (1961).
[18]W. T. Cronenwett and J. C. Thompson, Adv. Phys. 16, 439 (1967).
[19]R. B. Somoano and J. C. Thompson, Phys. Rev. A 1, 376 (1970).
[20]W. H. McKnight, and J. C. Thompson, Bull. Am. Phys. Soc. 17, 368 (1972); W. E. Mueller and J. C. Thompson, Proc. of Colloque Weyl II, edited by Lagowski and Sienko (Butterworths, London, 1970), p. 293.
[21]Morrel H. Cohen and J. Jortner, Phys. Rev. A 10, 978 (1974).
[22]N. F. Mott, *Metal–Nonmetal Transition* (Francis and Taylor, 1974).
[23]D. E. O'Reilly, J. Chem. Phys. 41, 3729 (1964).
[24]N. R. Kestner (private communication).
[25]D. W. Mahaffey and D. A. Jerde, Rev. Mod. Phys. 40, 710 (1968).
[26]R. L. Bush, Phys. Rev. (in press).
[27]A. S. Skal, Sov. Phys.–Solid State 16, 590 (1974).